

Electronic and Optical Properties of Double Perovskite Oxide $\text{Pb}_2\text{ScSbO}_6$: A First Principles Approach

Lalhriatpuia Hnamte¹, Himanshu Joshi¹ and R. K. Thapa^{1*}

¹Condensed Matter Theory Research Group, Department of Physics, Mizoram University, Aizawl- 796 004, INDIA

*Corresponding Author : r.k.thapa@gmail.com

Abstract : This paper reports the study of electronic and optical properties of double perovskite oxide $\text{Pb}_2\text{ScSbO}_6$ by using the FP-LAPW method within density functional theory. Lattice constants are calculated by doing volume optimisation. The values of bulk modulus and pressure derivatives have been obtained. Results of density of states and energy bands are also presented. The indirect band gaps have been found for both the systems by using the GGA and mBJ approximations. Calculations of optical properties are also presented by considering the variations of optical parameters as a function of incident photon energy.

Keywords : bands, density of states, double perovskite, FP-LAPW, photon energy, dielectric constants

Date of Submission: 20-05-2018

Date of acceptance: 05-06-2018

I. Introduction

Double perovskite compound with general formula $\text{AB}_2\text{B}'\text{O}_6$ (derived from simple ABO_3) where A represent alkaline-earth, rare earth or transition metals like Ba, Sr, Mn, Pb, etc. and B and B' represent transition metals like Fe, Mo, Co, W, V etc. [4,5,6]. Perovskite oxides were first studied in 1950, when ferromagnetic behavior is observed in manganites (AMnO_3 : A=divalent or trivalent cations) around room temperature [7]. Recent years, there had been a large number of strongly correlated investigation regarding on Pb-based double perovskite, $\text{Pb}_2\text{ScTaO}_6$ and $\text{Pb}_2\text{ScNbO}_6$ compounds is in paraelectric state at 400K and differs to ferroelectric phase at 4.2K and 200K by cooperative ion shift [8]. $\text{Pb}_2\text{ScNbO}_6$ (PSN) ceramics, a promising relaxor ferroelectric material, its powder mechanically activated at various pressures occur in different metastable structural states [9]. $\text{Pb}_2\text{YbNbO}_6$ at room temperature show antiferroelectric and upon when heating, it undergoes an antiferroelectric to paraelectric phase transition at 578 K [10, 11].

There had been a number of theoretical as well as experimental studies on 3d-5d double perovskite oxide. Also, amongst the double perovskites oxide, Sc-based compounds have attracted much attention because of their potential application in electronic and optical devices. Several such oxides have recently been synthesized and experimental studies have been performed over a wide range of temperature to understand their electronic structure and phase transition [12-14]. M. G. Brik had investigated the first principles calculations of electronic, optical and elastic properties of Ba_2MgWO_6 double perovskite [15]. Likewise, Zhe-Wen *et al.* studied perovskite oxide $\text{Bi}_2\text{FeCrO}_6$ and determined the antiferromagnetic behavior [16]. Recently, Ahmed studied Bi-based double perovskite oxides $\text{Bi}_2\text{FeMnO}_6$ and determine their magnetic, electronic and optical properties [17].

In the present work, we report on the first-principles study of electronic and optical properties of $\text{Pb}_2\text{ScSbO}_6$. To the best of our knowledge, up till now, there are no theoretical investigation reports relating on the electronic and optical properties of $\text{Pb}_2\text{ScSbO}_6$ in the literature. Thereby, the primary purpose of this work is to provide some additional information to the existing data on the physical properties of $\text{Pb}_2\text{ScSbO}_6$ with *ab-initio* calculations. We will apply here the method of full-potential linearized augmented plane wave (FP-LAPW) method within density functional theory (DFT) to study the electronic and optical properties.

II. Computational Details

We have performed the first principle calculations using the FP-LAPW method which is implemented in WIEN2k code [18] and based upon DFT [19]. In the FP-LAPW method, the solution to the Kohn Sham equations [20] are performed self-consistently and the augmented plane wave plus local orbital basis set is incorporated to represent the electronic band structure for all atoms and their corresponding orbitals. Here, the core states are treated fully relativistically while the semi-core and valence states are treated semi-relativistically. All the calculations were converged with respect to Brillouin zone (BZ) sampling and the size of the basis set. Brillouin zone (BZ) integrations within the self-consistency cycles were performed via a

tetrahedron method. The exchange and correlation effects have been treated within the three potential, Gradient approximation (GGA) [21] and modified Becke-Johnson exchange potential (mBJ) [22] based on the FP-LAPW method [23]. This method has been adopted by many authors [24, 25]. For a well conserved self-consistency cycle, an $20 \times 20 \times 20$ k-mesh was used in the first Brillouin zone, and the energy cut off was set to 10^{-5} Ry as suggested by previous literature [26]. The convergence parameter $R_{mt}K_{max}$, which controls the size of the basis sets, was set to 7 which determines matrix size (convergence), where K_{max} is the plane wave cut-off and R_{MT} is the smallest of all atomic sphere radii. The G_{max} parameter was taken to be 12 Bohr^{-1} .

III. Result And Discussions

3.1 Crystal structure: The double perovskite compound Pb_2ScSbO_6 crystallizes in cubic phase, forming face-centred cubic crystal structure ($Fm-3m$) with four atoms per unit cell. The atomic position in the unit cell are Pb (0.25, 0.25, 0.25), Sc (0.5, 0.5, 0.5), M (0, 0, 0) and O (0.2551, 0, 0), see figure 1. All internal atomic positions are in fractional coordinates. Fig 1 shows the (100) plane of the corresponding conventional unit cell which were displayed by using XCrySDen [27]. The structural optimization based on Murnaghan's equation of state [28] was performed to obtain the relax structure with minimum energy, the obtained optimized lattice parameters are summarized in Table I. Our calculated values of the lattice parameters are slightly higher than the available experimental data. This is usually expected for GGA as it tends to overestimate the lattice parameters. The structural optimization defines the obtained energy versus volume plot for Pb_2ScSbO_6 are given in fig. 2.

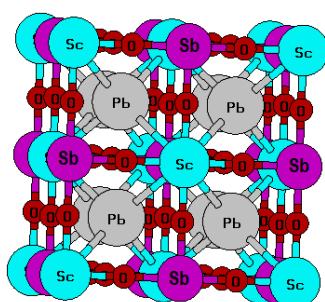


Fig. 1. Unit cell structure of double perovskite oxide Pb_2ScSbO_6

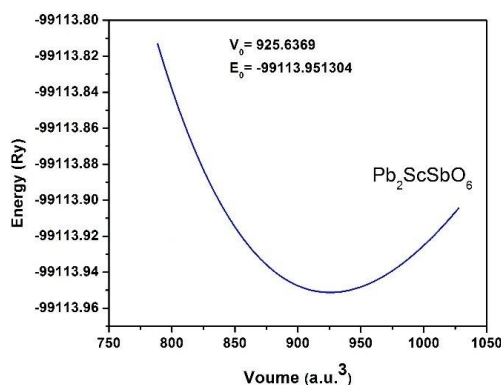


Fig. 2. Volume optimization of Pb_2ScSbO_6

Table 1. Calculated lattice constants, bulk modulus

Compound	Lattice constant Å		Ref.	Bulk B(GPa)
	Calculated (a)	Previous (a)		
Pb_2ScSbO_6	8.1866	8.1050	[35]	147.709

3.2 Electronic properties: The optimized lattice constants obtained after volume optimization were used to calculate the electronic structures of Pb_2ScSbO_6 . For better computation of the electronic states and the band gap of the compound, we have used the Generalized Gradient Approximation energy exchange correlation functional along with the modified Beck-Johnson potential, which is found to be very accurate for determination of band gaps of compounds, compared to GGA which tends to underestimate the band gap [29]. The electronic band structure of the double perovskite Pb_2ScSbO_6 are discussed and examined on the basis of total and partial density of states as shown in fig. 3

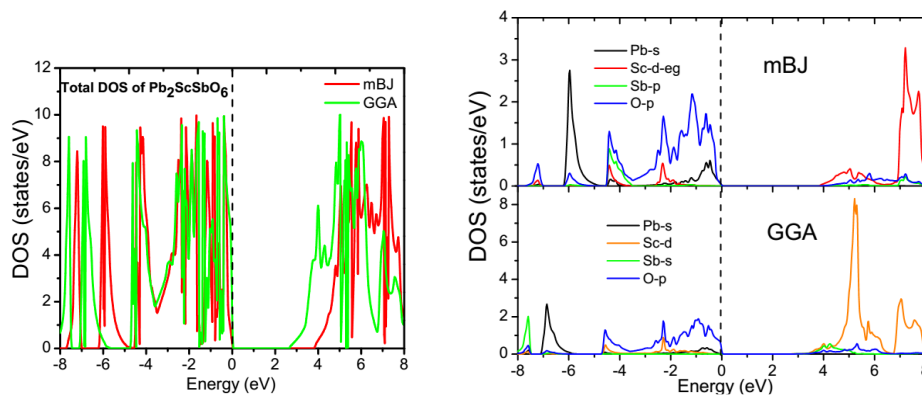


Fig. 3. Total and Partial DOS of Pb_2ScSbO_6

From figure 3 it can be seen that high DOS peaks dominates the valance band region as well as the conduction region, indicating availability of large number of states for occupation. At around the Fermi level (0 eV energy), the density of states is zero, meaning no states are available to be occupied.

The s states dominates the lower valance band region (-8 to -6 eV) with very low contribution from the p states of O atom. In the region between -6 eV to -4.8 eV, there are no available states for occupation as seen from GGA plot. The region decreases to -5 eV to -4.8 eV when treated with mBJ. The lower conduction region shows sharp peaks in case of GGA, but the contribution almost gets negligible in case of mBJ, which is the reason to open up a bigger band gap for mBJ treatment. The density of states and band structure of Pb_2ScSbO_6 are employed in order to understand the obtained electronic properties within GGA and mBJ potentials as shown in fig. 3 and 4. The GGA band structure and density of states result indicates that it is of semiconductor. The O-p states electron contribution are more in the valence region despite it does not have much impact in the hybridization between O-p states and Sc-d states near Fermi energy, the energy reference is selected to be the Fermi level in $E=0$. We can see many peaks at the valence region ranging from 0 to -8 eV, the majority contribution comes from s states of Pb and p states from O. High peak near Fermi energy in the valence band is contributed by O 2p states and peak near -6 eV is due to Pb 6s states. In the conduction region, the range between 3 to 10 eV, it was mainly contributes by d states from transition metals Sb. The basic covalent bond between Sc-4d to O-2p in Pb_2ScSbO_6 is to be mentioned that the maximum Sc- 4d contribution in Pb_2ScSbO_6 is zero at the valence band but significantly rises when increased the energy. The band structure of these materials along the various symmetry lines of Brillouin zone which shows the valence band near the Fermi level are derived from O-2p orbitals. It is clearly seen that the two compounds exhibit same type of band nature. From the band structure plot, it is seen that both the compound show that the bottom of conduction band and the top of valence band lies at X symmetry point and obtained that these two compounds is at X-X direct band gap. It means that a direct recombination takes place with the release of the energy equal to the energy difference between the recombining particles and also defines that the difference between the wave-vector is equal to zero. The efficiency factor of a direct band gap semiconductor is higher than those of indirect band. Therefore, these material is the best candidate for applications comprising the emission of photons through radiative recombination of electrons and holes and thereby, means that they are suitable for LED, lasers and optical sources. Since there is no experimental result to compare this theoretical results. As is well known, the band gap calculating using generalized gradient approximation (GGA) and local density approximation (LDA) are strongly underestimated in density functional theory based method due to their discontinuity [30].

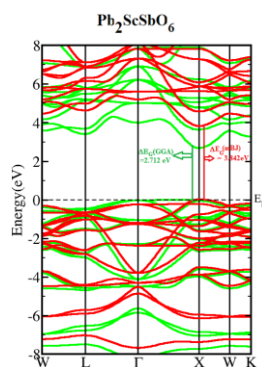


Fig. 4. Band structure plot for Pb_2ScSbO_6 (GGA green, mBJ red)

So in order to obtain efficient energy band gap values, modified Becke-Johnson potential (mBJ) was also employed, as this potential was perhaps the most suitable to produce accurate band gaps for different types of materials [31-38]. The electronic band structure plot for Pb₂ScSbO₆ are shown in fig. 4. Also the calculated direct energy band gap for these materials using the two correlation exchange GGA and mBJ are given in table 2.

Table 2. The theoretical calculated energy band gaps for Pb₂ScSbO₆

Compound	GGA (eV)	mBJ (eV)
Pb ₂ ScSbO ₆	2.712	3.842

3.3 Optical properties

From fig. 2(a) and (b), the band structure plot for these material conclude that it is a direct band at same symmetry point within GGA and mBJ potential. The knowledge of the obtained band gaps are further compared and examine with the optical properties. It is known that the optical properties of a solid can be described by the complex dielectric function $\epsilon(\omega)$, which have two parts real and imaginary can be expressed as [39]

$$\epsilon(\omega) = \epsilon_1(\omega) + i\epsilon_2(\omega) \tag{1}$$

From the electronic band structure of the material, the imaginary part $\epsilon_2(\omega)$ of the complex function $\epsilon(\omega)$ in cubic symmetry can be calculated as follows

$$\epsilon_2(\omega) = \left(\frac{\hbar^2 e^2}{\pi m^2 \omega^2} \right) \sum_{c,v} \int d^3k \langle c_k | p^\alpha | v_k \rangle \langle v_k | p^\beta | c_k \rangle x \delta(\epsilon_{c_k} - \epsilon_{v_k} - \omega) \tag{2}$$

Here, p represents the momentum matrix element between states of band α and β within the crystal momentum k. c_k and v_k are the crystal wave functions corresponding to the conduction and valence bands with crystal wave vector k. From the imaginary part using Kramers-Kronig relation, it gives the real part $\epsilon_1(\omega)$ of the dielectric function [40] as follows

$$\epsilon_1(\omega) = 1 + \frac{\pi}{2} p \int_0^\infty \frac{\omega' \epsilon_2(\omega')}{(\omega')^2 - \omega^2} d\omega' \tag{3}$$

Where p denotes the principal value of the integral. The real and imaginary parts of dielectric function allow us to gain the knowledge to obtain the primary importance of optical functions like the refractive index $n(\omega)$, extinction coefficient $k(\omega)$, absorption coefficient $\alpha(\omega)$ and reflectivity $R(\omega)$ are used given as follows [41].

$$n(\omega) = \frac{1}{\sqrt{2}} \left[\sqrt{\epsilon_1^2(\omega) + \epsilon_2^2(\omega)} + \epsilon_1(\omega) \right]^{\frac{1}{2}} \tag{4}$$

$$k(\omega) = \frac{1}{\sqrt{2}} \left[\sqrt{\epsilon_1^2(\omega) + \epsilon_2^2(\omega)} - \epsilon_1(\omega) \right]^{\frac{1}{2}} \tag{5}$$

$$\alpha(\omega) = \sqrt{2} \omega \left[\sqrt{\epsilon_1^2(\omega) + \epsilon_2^2(\omega)} - \epsilon_1(\omega) \right]^{\frac{1}{2}} \tag{6}$$

$$R(\omega) = \left| \frac{\sqrt{\epsilon(\omega)} - 1}{\sqrt{\epsilon(\omega)} + 1} \right|^2 \tag{7}$$

The variation of the calculated dielectric function, absorption coefficient, refractive index and reflectivity for Pb₂ScSbO₆ as a function of photon energy with GGA and mBJ are shown in Fig. 5.

Table 3. The calculated dielectric constant $\epsilon_1(\omega)$, absorption coefficient $\alpha(\omega)$, refractive index $n(\omega)$ and reflectivity $R(\omega)$ (in arbitrary unit)

Compound	GGA				mBJ			
	$\epsilon_1(\omega)$	$\alpha(\omega)$	$n(\omega)$	$R(\omega)$	$\epsilon_1(\omega)$	$\alpha(\omega)$	$n(\omega)$	$R(\omega)$
Pb ₂ ScSbO ₆	5.80	2.70	2.42	0.17	4.10	3.75	2.04	0.12

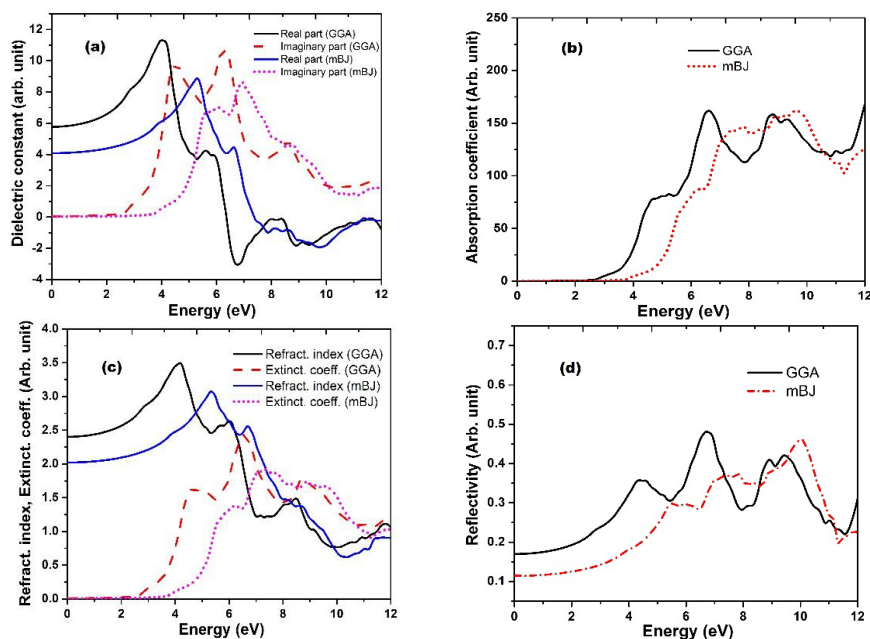


Fig. 5. Dielectric constant, (b) absorption coefficient, (c) refractive index and (d) reflectivity of Pb_2ScSbO_6

The compounds Pb_2ScSbO_6 under investigations are having cubic symmetry. Since in cubic symmetry we have the principal tensor component $\epsilon_{xx} = \epsilon_{yy} = \epsilon_{zz}$, therefore we have to calculate only one component of the complex dielectric function. Hence, the variations in real and imaginary (absorption) parts of the complex dielectric function (ϵ_0) for the Pb_2ScSbO_6 within GGA and mBJ are given in Fig. 5. The analysis of Fig. 5 shows that, the calculated real parts of the dielectric function for Pb_2ScSbO_6 are 5.80 (GGA), 4.10 (mBJ). The imaginary part from Fig. 5 shows the first optical critical point of the complex dielectric function which occurs for Pb_2ScSbO_6 at 2.50 eV (GGA), 3.65 eV (mBJ). This point indicates the $X_v - X_c$ splitting, which shows the threshold of optical direct transition between the lowest of the conduction band and the highest of the valence band and is also known as the absorption edge. Above this point, with the increase of the energy, we have seen that the curve increases along. It is because the real part of the dielectric function increases instantaneously. The reason behind the occurrence of rapid peak in the optical spectrum is that the transition between the occupied states from the valence region to the unoccupied states from the conduction region. From mBJ compare to GGA, the main peak of the real and imaginary parts shifted due to increase of energy. From Fig. 5, the resulted peak in the absorption plots quite similar to the peak of imaginary parts of the complex dielectric function, which follows the linear absorption spectra is originated from the imaginary parts of the electronic dielectric function. From energy range 0 eV to 12 eV, we have obtained a peaks at energy of 4.5 (GGA), 5.7 (mBJ); 5.1 (GGA), 7.02 (mBJ); 6.8 eV (GGA), 7.9 (mBJ) and 7.8 (GGA), 8.6 (mBJ). From the absorption spectra, we have seen that as energy decreases the absorption coefficient decreases rapidly, which should be the behavior of common semiconductors.

IV. Conclusion

First principles calculation have been employed to study the electronic structure and optical properties of double perovskite Pb_2ScSbO_6 using full potential linearized augmented plane wave method under generalized gradient approximations within Wien2k. The calculated electronic properties showed Pb_2ScSbO_6 to be semiconductor and showed that it is of direct band as the lowest energy in conduction and highest band in the valence region lies in X-X symmetry was observed. The optical properties also indicate a possible application of Pb_2ScSbO_6 in LED devices

Acknowledgements

LH thanks Mizoram University for a fellowship and HJ and RKT acknowledges a grant from SERB vide No, EMR/2015/001407, Dt.10-08-2016.

References

- [1]. H. Y. Hwang, S. W. Cheong. Low-field magneto-resistance in the pyrochlore $Tl_2Mn_2O_7$. Nature (London) 389, 1997, 942.
- [2]. D. Serrate, J. M. D. Teresa, M. R. Ibarra. Double perovskites with ferromagnetism above room temperature. J. Phys. Condensed Matt. 19, 2007, 023201.

- [3]. A. J. Hauser, J. R. Soliz, M. Dixit, R. E. A. Williams, M. A. Susner, B. Peters, L. M. Mier, T. L. Gustafson, M. D. Sumption, H. L. Fraser, P. M. Woodward and F. Y. Yang. Fully ordered Sr₂CrReO₆ epitaxial films: A high-temperature ferrimagnetic semiconductor. *Phys. Rev. B* 85, 2012, 161201.
- [4]. K. I. Kobayashi, T. Kimura, H. Sawada, K. Terakura, Y. Tokura. *Nature* 395, 1998, 677–680.
- [5]. M. Bonin, W. Paciorek, K. Schenk, G. Chapuis. *Acta Crystallogr., Sect. B: Struct. Sci.* 51, 1995, 48.
- [6]. M. Saad. Promising half-metallic ferromagnetism in double perovskites Ba₂VTO₆ (T= Nb and Mo): Ab initio LMTO ASA investigations, *Solid State Communications* (2012) <http://dx.doi.org/10.1016/j.ssc.2012.04.031>.
- [7]. G. H. Jonker, J. H. van Santen. Ferromagnetic compounds of manganese with perovskite structure, *Physica*, 16, 1950, 337.
- [8]. K. Z. B. Kishi, P. M. Woodward, K. Knight. The crystal structures of Pb₂ScTaO₆ and Pb₂ScNbO₆ in the paraelectric and ferroelectric states, *Ferroelectrics*, 261(1), 2001, 21-26.
- [9]. E. N. Ubushaeva, E. V. Likhushina, K. G. Abdulvakhidov, M. A. Vitchenko, B. K. Abdulvakhidov, V. B. Shirokov, N. V. Lyanguzov, Yu. I. Yuzyuk, E. M. Kaidashev, I. V. Mardasova. Published in *Pis'ma v Zhurnal Tekhnicheskoi Fiziki*, Vol. 37, No. 20, 2011, pp. 23–31.
- [10]. V. A. Isupov, N. N. Krainik. *Phys. Solid State*, 6, 1965, 2975.
- [11]. J. R. Kwon, W. K. Choo. *J. Phys.: Condens. Matter*, 3, 1991, 2147
- [12]. A. Faik, J. M. Iguarta, M. Gateshki, G. J. Cuello. *Jour. of Solid State chem.* 182, 2009, 1717.
- [13]. A. Faik, D. Orobengoa, E. T. Zabola, J. M. Iguarta. *Journ of Solid State Chem.* 192, 2012, 273.
- [14]. A. Dutta, T. P. Sinha. *Journ. of Phys. & Chem. Of Solids* 74, 2013, 250.
- [15]. E. N. Brik. *Journal of Physics and Chemistry of Solids* 73, 2012, 252–256.
- [16]. Z. W. Song, B. G. Lui. *Chin. Phys. B* Vol. 22, No. 4, 2013, DOI: 10.1088/1674-1056/22/4/047506.
- [17]. T. Ahmed, A. Chen, D. A. Yarotski, S. A. Trugman, Q. Jia, J. X. Zhu. *APL Mater.* 5, 035601, 2017, DOI: 10.1063/1.4964676.
- [18]. P. Blaha, K. Schwarz, G.K.H. Madsen, D. Kvasnicka, J. Luitz. WIEN2K, An Augmented Plane Wave Plus Local Orbitals Program for Calculating Crystal Properties (2001) (Vienna: Vienna University of Technology).
- [19]. P. Hohenberg, W. Kohn. *Phys. Rev.* 136, 1964, 864-871.
- [20]. W. Kohn, L. J. Sham. Self-consistent equations including exchange and correlation effects. *Phys. Rev.*, 140, 1965, A1133.
- [21]. J. P. Perdew, K. Burke, M. Ernzerhof. *Phys. Rev. Lett.* 77, 1996, 3865.
- [22]. J. P. Perdew, Y. Wang. *Phys. Rev. B* 45, 1992, 13244.
- [23]. F. Tran, P. Blaha. *Phys. Rev. Lett.* 102, 2009, 226401.
- [24]. Himanshu Joshi, Dibya P Rai, R. K. Thapa, AIP Conference Proceedings, 1942, 2018, 110056.
- [25]. Lalhriatpuia Hnamte, Sandeep .Himanshu Joshi and R. K. Thapa, AIP Conference Proceedings, 1953, 2018, 140132.
- [26]. H. J. Monkhorst, J.D. Park. *Phys. Rev. B* 13, 1976, 5188.
- [27]. A. Kokalj. X-CrysDen. X-Window Crystalline Structures and Densities. *Comp. Mater. Sci.*, Vol. 28, 2003, p. 155.
- [28]. F. D. Murnaghan. *Proc. Natl. Acad. Sci. USA*, 1994, 30.
- [29]. F. Galasso. *Perovskites and High Tc superconductors*, (Gordon & Breach, New York, 1990).
- [30]. Agostino Zoroddu, Fabio Bernardini and Paolo Ruggerone, *PHYSICAL REVIEW B*, 64, 2001, 045208.
- [31]. J. P. Perdew, R. G. Parr, M. Levy, J.L. Balduz. *Phys. Rev. Lett.* 49, 1982, 1691.
- [32]. D. J. Singh. *Phys. Rev. B* 82, 2010, 205102.
- [33]. S. D. Guo, B. G. Liu. *J. Appl. Phys.* 110, 2011, 073525.
- [34]. S. D. Guo, B. G. Liu. *Europhys. Lett.* 93, 2011, 47006.
- [35]. D. J. Singh. *Phys. Rev. B* 82, 2010, 155145.
- [36]. D. J. Singh, S. S. A. Seo, H.N. Lee. *Phys. Rev. B* 82, 2010, 180103.
- [37]. S. D. Guo, B. G. Liu. *J. Phys. Condens. Matter.* 24, 2012, 045502.
- [38]. S. D. Guo, B. G. Liu. *Chin. Phys. B* 21, 2012, 017101.
- [39]. C. A. Draxl, J. O. Sofo. Linear optical properties of solids within the full-potential linearized augmented planewave method, *Computer Physics Communications*, 175(1), 2006, 1 – 14.
- [40]. M. P. Fox. *Optical Properties of Solids*, 2nd edn. (Oxford University Press, Oxford, 2001) p. 31.
- [41]. A. Delin, O. Eriksson, R. Ahuja, B. Johansson, M.S.S. Brooks, T. Gasche, S.Auluck and J. M. Wills. *Phys. Rev. B* 54, 1996, 1673.

IOSR Journal of Applied Physics (IOSR-JAP) (IOSR-JAP) is UGC approved Journal with Sl. No. 5010, Journal no. 49054.

Lalhriatpuia Hnamte. " Electronic And Optical Properties of Double Perovskite Oxide Pb₂Sc Sb O₆: First Principles Approach." IOSR Journal of Applied Physics (IOSR-JAP) , vol. 10, no. 3, 2018, pp. 39-44.